

# SIMULATION OF TECHNOLOGICAL PROCESS BY USAGE NEURAL NETWORKS AND FACTORIAL DESIGN OF EXPERIMENTS

ALENA VAGASKA<sup>1</sup>, PETER MICHAL<sup>2</sup>, MIROSLAV GOMBAR<sup>3</sup>,  
ERIKA FECHOVA<sup>1</sup>, JAN KMEC<sup>3</sup>

<sup>1</sup>Technical University of Kosice, Faculty of Manufacturing Technologies with a seat in Presov, Slovak Republic

<sup>2</sup>CCTo, Presov, Slovak Republic

<sup>3</sup>Institute of Technology and Businesses in Ceske Budejovice, Czech Republic

DOI: 10.17973/MMSJ.2016\_09\_201662

e-mail: alena.vagaska@tuke.sk

The possibilities of simulation of technological process of aluminium anodic oxidation using the methodology of Design of Experiments (DOE) and theory of neural networks in order to monitor the anodizing process under various operating conditions are presented in this paper. The influence of chemical and physical input factors on the resulting AAO (anodic aluminium oxide) layer thickness at applied current density of 1 A·dm<sup>-2</sup> and 6 A·dm<sup>-2</sup> has been investigated. Based on the evaluation of experimentally obtained data, the computational predictive model describing the effect of individual input factors and their mutual interactions on the AAO layer thickness was developed in the form of cubic function. This model indicates which factors are important and how they combine to influence the response, it will enable us to optimize operating conditions. The most significant benefit of our research work in this field is the fact that all relevant factors were varied simultaneously.

## KEYWORDS

*design of experiments, neural unit, predictive model, anodizing, layer thickness, factors*

## 1 INTRODUCTION

Aluminum and its alloys are common materials for manufacturing due to its properties (low density, high mechanical strength, good conductivity, corrosion and wear resistance, etc.). It is commonly used in the aerospace and automotive industries, for building materials, domestic products, packaging and electrical applications [Baumeister 1997, Dobrzanski 2005]. Anodic aluminium oxide (AAO) coatings have recently attracted the scientists' attention because of their usefulness and wide range of applications [Rahimi 2009]. Anodizing is one of the most important processes in corrosion protection and colour finishes for aluminium [Tsangaraki-Kaplanogloua 2006 a], it is an effective process applied to produce decorative and protective films on articles made from aluminium [Djozan 2003]. During the process of aluminium anodic oxidation different type of the electrolyte are used, the most frequently used are sulphuric acid and oxalic acid, alternatively a combination of them, because of their environmental friendliness [Badida 2013]. The mechanism of an oxide layer formation when using sulphuric acid solution has been observed in many studies, for example in [Tsangaraki-Kaplanogloua 2006 b, Patermarakis 1998, Aerts

2009] researchers were focused to design a mathematical model of local turbulences in the electrolyte and examine their influence on the geometrical dimensions of the pores. Other studies were also dealing with the temperature effect on the growth of the oxide layer [Aerts 2010] and the layer porosity [Aerts 2007] of 99.50 % aluminium using the electrolyte comprising sulphuric acid based on which it followed that the structure of the layer, the layer porosity, its thickness and hardness are not so much under the influence of the temperature of the electrolyte compared to that of the electrode.

Despite the information available in literature on the influence of the operating conditions (input factors) on the response (the thickness of the formed oxide layer), studies which consider all relevant factors at a time are rare. The usage of DOE methodology to construct a carefully prepared set of experiments is one of the basic tools which helps us to show the influence of input variables (varied simultaneously) on outputs (responses) [Gombar 2014, Box 2008]. The optimum selection of process conditions is an extremely important issue as these determine surface quality of the manufactured components [Gombar 2014]. The mathematical modelling of the anodizing process involves several parameters that may lead to difficult analytical solution [Box 2008] On the other hand, the usage of artificial intelligence for evaluation of experimental results has its merits. Mainly because of one obtains more useful and more precise information about the studied system, the predictive model of the studied process will be more reliable and can be developed faster in comparison with usage only classical statistical methods [Panda 2016, Hrehova 2013]. Also it is possible to achieve maximum output or minimum input or both by usage appropriate type of neural unit order and learning algorithm [Bukovsky 2013].

## 2 EXPERIMENTAL

Specimens of aluminium alloys EN AW 1050 - H24 with dimensions 101 x 70 x 1 mm were used. The specimens had undergone the following pre-treatments: degreasing in a 38 % solution of NaOH at 55 to 60 °C for 2 minutes and etching in a 40 % solution of NaOH at the temperature 45 – 50 °C for 0.50 min. Consequently, the specimens were immersed for 1 minute in a nitric acid bath (4 % HNO<sub>3</sub>) at the temperature 18 to 24 °C. Between each operation, the samples were rinsed thoroughly in deionized water. The anodizing process was carried out in the electrolyte containing sulphuric acid, oxalic acid, boric acid and sodium chloride. Their concentrations were determined according to the DOE using a central composite design for seven input factors and four levels of each, the center of the experimental region have been added. The operating conditions (electrolyte temperature, anodizing time and applied voltage) also were determined on the basis of central composite design. The actual design matrix of experiment was created, individual test runs were performed on the basis of this design matrix created as a combination of individual levels of seven investigated factors. Table 1 shows the individual levels of investigated factors in coded scale and natural one. Coded scale is used to prevent influence of the absolute term of the studied factor in evaluating the results of the experiment. By means of DOE, individual runs were performed in random order to eliminate systematic error and to avoid subjective preference of any factor-level. Use scalar products the orthogonality of experiment design were verified. The thickness of the resulting AAO layer was measured in the defined experimental points by usage of digital thickness meter. Experimental points were indicated at the intersections

of horizontal and vertical lines, distance between individual lines and from the bottom edge of the sample was 5 mm. The layer thickness was measured five times at each experimental point. The arithmetic average of five measurements was taken as an individual measurement.

Coded scale	Natural scale	Factor level				
		-2.83	-1	0	1	2.83
$x_1$	$\text{H}_2\text{SO}_4[\text{g}\cdot\text{l}^{-1}]$	12.57	40.00	55.00	70.00	97.43
$x_2$	$\text{C}_2\text{H}_2\text{O}_4[\text{g}\cdot\text{l}^{-1}]$	3.76	6.50	8.00	9.50	12.24
$x_3$	$\text{H}_3\text{BO}_3[\text{g}\cdot\text{l}^{-1}]$	4.51	10.00	13.00	16.00	21.49
$x_4$	$\text{NaCl}[\text{g}\cdot\text{l}^{-1}]$	0.12	0.30	0.40	0.50	0.68
$x_5$	$T[^\circ\text{C}]$	-5.46	11.00	20.00	29.00	45.46
$x_6$	$U[\text{V}]$	2.34	6.00	8.00	10.00	13.66
$x_7$	$t[\text{min}]$	1.72	20.00	30.00	40.00	58.28

Table 1. Levels of observed factors

### 3 METHODS OF DATA EVALUATION

Experimentally obtained data were evaluated by methods of statistical analysis and methods of artificial intelligence. The multiple linear regression (MLR) and theory of neural units, especially Levenberg-Marquardt (LM) algorithm, were applied to the modelling of effects of observed input factors on the response in order to obtain the computational predictive model. Before applying regression analysis on the experimentally obtained data, the DOE standardization (coding) of input factors into coded unit was performed to obtain correct statistical significance of regression coefficients [Hrehova 2013a, Erikson 2008, Gombar 2014, Box 2008]. Based on the statistical analysis of experimentally obtained data (screening analysis, analysis of variance ANOVA, DOE analysis) using software such as Matlab, Statistica, QC-Expert [Krenicky 2011, Hrehova 2013b, Murcinkova 2013], we have indicated important factors affecting the final layer thickness, we analysed how they interact and obtained computational statistical models predicting the value of thickness. Levenberg-Marquardt (LM) algorithm is described by equation (1) – equation (8). It is a process of updating individual weights  $w$  in a predetermined number of steps to achieve a minimum difference between the real (measured) and calculated values [Gupta 2012]. The vector  $u$  of neural inputs is created by taking the partial derivatives of each output in respect to each weight equation (1) – equation (3). The equation describing the investigated model is the characteristic equation of given type of neural unit for observed factors  $x_1, x_2, x_3, x_4, x_5, x_6$  and  $x_7$ .

$$u_i = \frac{\partial y_{HONU}}{\partial w_i} \quad (1)$$

$$u = \begin{bmatrix} u_1 \\ u_2 \\ \vdots \\ u_n \end{bmatrix} \quad (2)$$

$$w = \begin{bmatrix} w_1 \\ w_2 \\ \vdots \\ w_n \end{bmatrix} \quad (3)$$

The Levenberg-Marquardt algorithm consists in solving equation (4), where the Jacobian  $J$  is the matrix of dimension  $m \times n$ ,

where  $n$  is the length of the input vector  $u$  of the neural unit ( $n$  is the number of neural inputs) and  $m$  is the total number of parameters intended for the learning procedure. The vector of neural inputs as well as the Jacobian is defined in the first step of the learning procedure and they remain constant in all subsequent steps of learning.

$$J = \begin{bmatrix} u_1^T \\ u_2^T \\ \vdots \\ u_m^T \end{bmatrix} = \begin{bmatrix} u_{1,1} & u_{2,1} & \cdots & u_{n,1} \\ u_{1,2} & u_{2,2} & \cdots & u_{n,2} \\ \vdots & \vdots & \ddots & \vdots \\ u_{1,m} & u_{2,m} & \cdots & u_{n,m} \end{bmatrix} \quad (4)$$

The vector  $y'$  of neural outputs is defined as the vector product of vectors  $w$  and  $u$  (equation (5)):

$$y' = w \times u \quad (5)$$

The size of the individual weight is set in the first step randomly. After calculating the output vector the error vector  $e$  is calculated as the difference between the actual value  $y$  of the observed variable and the calculated one by the neural units  $y'$  (equation (6)):

$$e = y - y' \quad (6)$$

Then the weight update vector  $\Delta w$  is determined by equation (7). In equation (7) there is the weight update vector  $\Delta w$  that we want to find,  $e$  is the error vector containing the output errors for each input vector used on training the network,  $1/\mu$  is the Levenberg's damping factor which tells us how much we should change our network weights to achieve a (possibly) better solution. The  $J^T \cdot J$  matrix can also be known as the approximated Hessian, the  $I$  is an identity matrix of diagonal length equal to the number of neural weights (matrix of dimension  $n \times n$ ), and  $\mu$  is the learning rate. The size of the learning rate  $\mu$  depends on how quickly and how accurately the neural unit is able to learn. At higher values of learning rate the neural unit will learn faster but there is a risk of instability respectively a risk of model oscillation. At lower values of learning rate the calculation is more accurate but the learning process requires a larger number of iterations [Bukovsky 2013].

$$\Delta w = \left( J^T \cdot J + \frac{1}{\mu} \cdot I \right)^{-1} \cdot J^T \cdot e \quad (7)$$

After calculating the weight-updates equation (8), the adaptation of the weights of input factors  $w_n$  occurs. Vector of weights update  $\Delta w$  is sum up to actual vector of weight  $w_{n-1}$ , where  $n$  is number of actual iterations. This is the end of iteration loop for the learning process of neural unit using iterative Levenberg-Marquardt algorithm optimization. The learning process of neural units continues by calculating the vector of neural outputs  $y$  using the new (adapted) weights.

$$w_n = w_{n-1} + \Delta w \quad (8)$$

### 4 RESULTS AND DISCUSSION

When the learning process of neuron unit was done, we obtained a computational model in the form of equation (9) and equation (10), which is describing and predicting the final thickness of AAO layer formed during anodizing process at surface current density of  $1 \text{ A}\cdot\text{dm}^{-2}$ . The thickness of AAO layer formed during anodizing process at surface current density of  $6 \text{ A}\cdot\text{dm}^{-2}$  is expressed by equation (11) and equation (12).

$$th_{j1} = \frac{3}{1 + e^{-aj1}} \cdot 3 \cdot std_{y,j1} \quad (9)$$

$$\alpha_{j1} = \sum_{i=1}^n (u_{ij1} \cdot w_{ij1}) \quad (10)$$

$$th_{j6} = \frac{3}{1 + e^{-\alpha_{j6}}} 3 \cdot std_{y_{j6}} \quad (11)$$

$$\alpha_{j6} = \sum_{i=1}^n (u_{ij6} \cdot w_{ij6}) \quad (12)$$

Where  $th$  is the final thickness of oxide layer,  $\alpha$  is preliminary thickness of oxide layer,  $u_i$  is a combination of input factors levels (in coded scale) and  $w_{j1}$  and  $w_{j6}$  are weights of combinations of their respective input factors. Calculated thickness of oxide layer is expressed in  $\text{mm} \cdot 10^{-3}$ .

We have chosen 36 randomly measured values of the final thickness and used them to develop predictive models of AAO layer thickness formed at applied current density of  $1 \text{ A} \cdot \text{dm}^{-2}$ . Figure 1 shows results of training process as comparison of measured and predicted thicknesses of AAO layer at current density of  $1 \text{ A} \cdot \text{dm}^{-2}$ . We can see that all values are situated closely to straight line of ideal prediction (error free prediction). It means that neural units were able to develop training models with high precision.

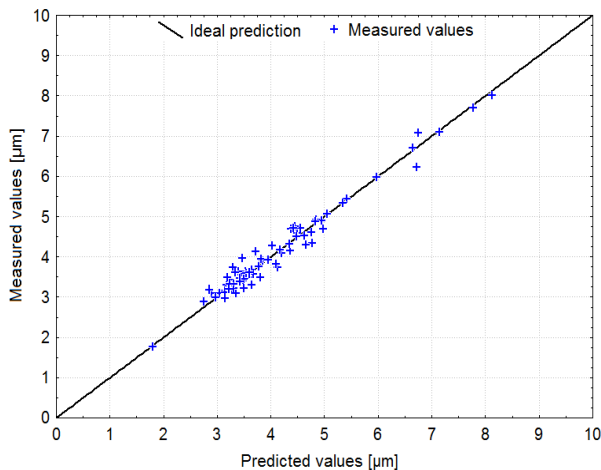


Figure 1. Results of training process for current density of  $1 \text{ A} \cdot \text{dm}^{-2}$

We have used remaining 44 measured values to validate the prediction model of AAO layer thickness for current density of  $1 \text{ A} \cdot \text{dm}^{-2}$ . Figure 2 shows the results of validation as comparison of measured and predicted thicknesses of AAO layer formed at current density of  $1 \text{ A} \cdot \text{dm}^{-2}$ .

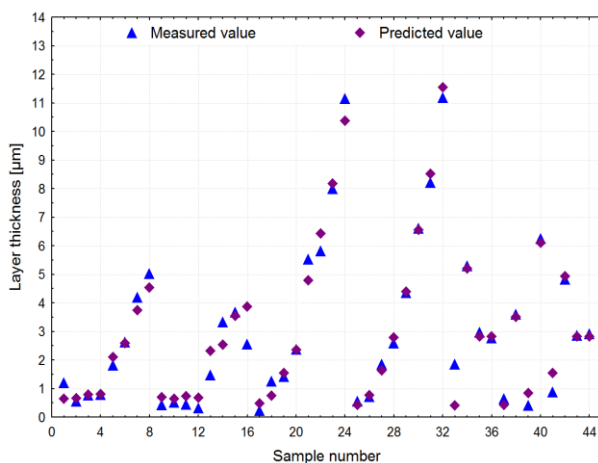


Figure 2. Validation of model reliability for current density of  $1 \text{ A} \cdot \text{dm}^{-2}$

It can be seen that values not used during training process (purple squares) are usually approaching to measured values (blue triangles). All of predicted values are situated close to corresponding measured values. It means that the prediction model is not error free but it is enough reliable to predict untrained values.

Process of validation continues with validation of accuracy of prediction model. Other 44 samples with different electrolyte composition and with different operating conditions were anodized. For these 44 samples the layer thickness by developed predictive model was calculated. Figure 3 shows the differences between the measured and predicted values. It can be seen that the error of predicted layer thickness is up to  $\pm 1 \mu\text{m}$ . This error is presented only six times. In other thirty eight cases the error of prediction is up to  $\pm 0.5 \mu\text{m}$ . This means that developed predictive model is reliable with high accuracy and it is possible to use it to monitor the relationship between operating parameters and created layer thickness of aluminium oxide.

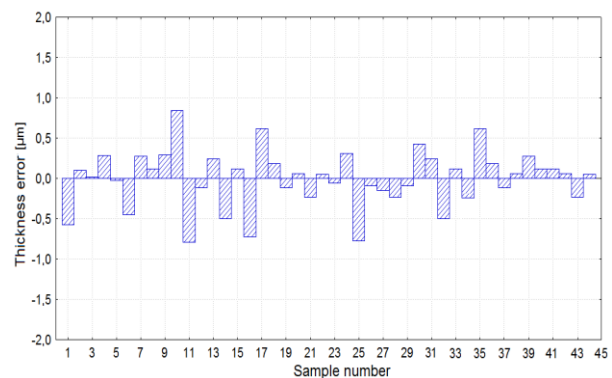


Figure 3. Validation of model accuracy for current density  $1 \text{ A} \cdot \text{dm}^{-2}$

If we obtain the model which describes the examined process we are able to monitor the influence of input factors on resulting layer thickness of aluminium oxide.

Figures 4, Figure 5, Figure 6 and Figure 7 show the influence of input factors on AAO layer thickness formed during anodizing process at current densities of  $1 \text{ A} \cdot \text{dm}^{-2}$ .

Figure 4 shows the influence of concentration of sulphuric acid in electrolyte on the resulting layer thickness along different concentration of sodium chloride in electrolyte. Concentration of oxalic acid is  $8 \text{ g} \cdot \text{l}^{-1}$ , concentration of boric acid is  $13 \text{ g} \cdot \text{l}^{-1}$ , electrolyte temperature is  $20 \text{ }^\circ\text{C}$ , applied voltage is  $8 \text{ V}$  and anodizing time is  $30 \text{ min}$ .

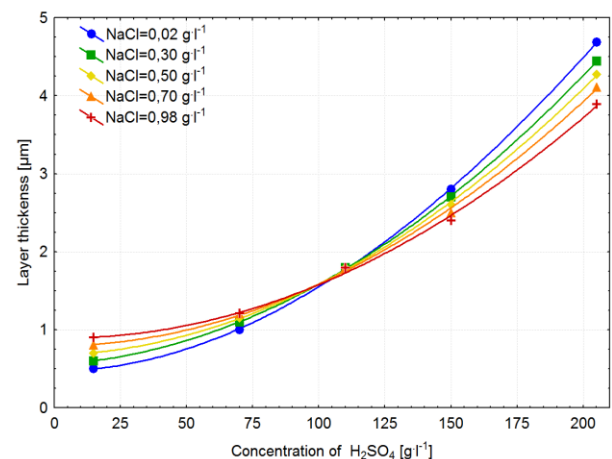


Figure 4. Influence of  $\text{H}_2\text{SO}_4$  cross NaCl on the layer thickness at current density of  $1 \text{ A} \cdot \text{dm}^{-2}$

Figure 5 shows the influence of concentration of oxalic acid in electrolyte on the resulting layer thickness along different concentration of boric acid in electrolyte. Concentration of sulphuric acid is  $55 \text{ g}\cdot\text{l}^{-1}$ , concentration of sodium chloride is  $0.4 \text{ g}\cdot\text{l}^{-1}$ , electrolyte temperature is  $20 \text{ }^\circ\text{C}$ , applied voltage is  $8 \text{ V}$  and anodizing time is  $30 \text{ min}$ .

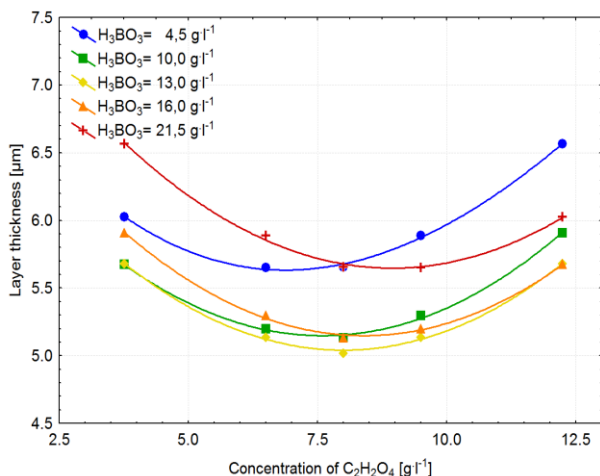


Figure 5. Influence of  $\text{C}_2\text{H}_2\text{O}_4$  cross  $\text{H}_3\text{BO}_3$  on the layer thickness at current density of  $1 \text{ A}\cdot\text{dm}^{-2}$

Figure 6 shows the influence of electrolyte temperature on resulting layer thickness along different concentration of boric acid in electrolyte. Concentration of sulphuric acid is  $55 \text{ g}\cdot\text{l}^{-1}$ , concentration of oxalic acid is  $8 \text{ g}\cdot\text{l}^{-1}$ , concentration of sodium chloride is  $0.4 \text{ g}\cdot\text{l}^{-1}$ , applied voltage is  $8 \text{ V}$  and anodizing time is  $30 \text{ min}$ .

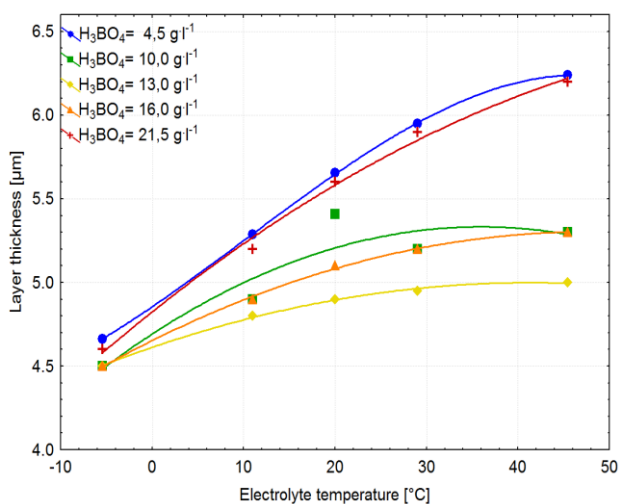


Figure 6. Influence of  $T$  cross  $\text{H}_3\text{BO}_3$  on the layer thickness at current density of  $1 \text{ A}\cdot\text{dm}^{-2}$

Figure 7 shows the influence of applied voltage on resulting layer thickness along different concentration of sodium chloride in electrolyte. Concentration of sulphuric acid is  $55 \text{ g}\cdot\text{l}^{-1}$ , concentration of oxalic acid is  $8 \text{ g}\cdot\text{l}^{-1}$ , concentration of boric acid is  $13 \text{ g}\cdot\text{l}^{-1}$  and anodizing time is  $30 \text{ min}$ .

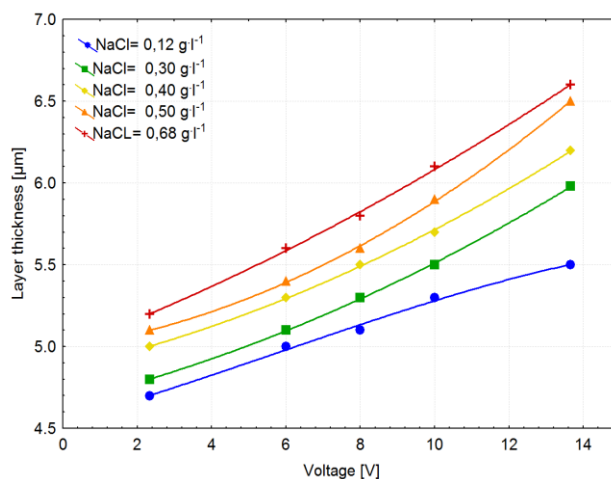


Figure 7. Influence of  $U$  cross  $\text{NaCl}$  on the layer thickness at current density of  $1 \text{ A}\cdot\text{dm}^{-2}$

## 5 CONCLUSION

In contrast to common experiments in this field of research of anodizing process, where is considered manipulating of only one factor at a time and its impact on the response, in our work we focused on the influence of all relevant factors and their interactions. The application of DOE is very useful for this purpose, whereby all such factors are manipulated simultaneously and fewer experiments are required. Also the application of neural networks theory is very important and useful for evaluation of experimental results to create a simulation model of technological process. Usage of higher order of neural unit based on the iterative Levenberg-Marquardt optimization algorithm provides a wide range of options to describe the examined process and investigate the influence of input factors on AAO layer thickness. The simulation model with reliability of  $99.37\%$  and accuracy up to  $\pm 1 \text{ }\mu\text{m}$  for current density of  $1 \text{ A}\cdot\text{dm}^{-2}$  was obtained. Such a high reliability and accuracy offer possibilities for optimization of the examined technological processes. The usage of developed simulation model allows us to reduce the operating costs and simultaneously create desired value of AAO layer thickness. The results obtained by our experimental work have important benefits for technical practice, because they were practically verified under conditions of real production.

## ACKNOWLEDGMENT

The research work was supported by grant VEGA 1/0738/14 "The Study of Corrosion Resistance of Coated Steel Sheets for Use in Automotive Industry" of the Scientific Grant Agency of the Ministry of Education of the Slovak Republic and by grant KEGA 026TUKE-4/2016.

## REFERENCES

- [Aerts 2007] Aerts, T. et al. Influence of the anodizing temperature on the porosity and the mechanical properties of the porous anodic oxide film. *Surface & Coatings Technology*, 2007, Vol. 201, pp. 7310 – 7317.
- [Aerts 2009] Aerts, T. et al. Experimental study and modelling of anodizing of aluminium in a wall-jet electrode set-up in laminar and turbulent regime. *Corrosion Science*, 2009, Vol. 51, pp. 1482 – 1489.
- [Aerts 2010] Aerts, T., DeGraeve, I., Nelissen, G. Comparison between the influence of applied electrode and electrolyte

- temperatures on porous anodizing of aluminium. *Electrochimica Acta*, 2010, Vol. 55, pp. 3957 – 3965.
- [Badida 2013] Badida, M. et al. The influence of sodium chloride on the resulting AAO film thickness. In: *Advanced Materials Research*, 2013, Vol. 816-817, pp. 18 – 22.
- [Baumeister 1997] Baumeister, J., Banhart, J., Weber, M. Aluminium foams for transport industry. In: *Materials & Design Journal*, 1997, Vol. 18, pp. 217 – 220.
- [Box 2008] Box, G. E. P., Hunter, J. S., Hunter, W. G. *Statistics for Experimenters*. New Jersey: John Wiley and Sons, 2008, pp. 639. ISBN 978-0-471-71813-0
- [Bukovsky 2013] Bukovsky, I. Learning entropy: multiscale measure for incremental learning. *Entropy*, 2013, Vol. 10, pp. 4159 – 4187.
- [Djozan 2003] Djozan, Dj., Amir-Zehni, M. Anodizing of inner surface of long and small-bore aluminum tube. *Surface & Coatings Technology*, 2003, Vol. 173, pp. 185 – 191.
- [Dobrzanski 2005] Dobrzanski, L. A. et al. Computer aided classification of flaws occurred during casting of aluminium. *Journal of Materials Processing Technology*, 2005, Vol. 167, pp. 456 – 462.
- [Eriksson 2008] Eriksson, L. et al. *Design of Experiments*. Umetrix Academy, 2008, pp. 459. ISBN 10-91-973730-4-4
- [Gombar 2014] Gombar, M. et al. The simulation of the temperature effects on the microhardness of anodic alumina oxide layers. *Metalurgija*, 2014, Vol. 53, pp. 59 – 62.
- [Gupta 2012] Gupta, M. M. et al. Fundamentals of higher order neural networks for modeling and simulation. In: *Artificial Higher Order Neural Networks for Modeling and Simulation*, ed. M. Zhang. Hershey, PA: IGI Global, 2012, pp. 103-133
- [Hrehova 2013a] Hrehova, S., Mizakova, J. Evaluation a process using fuzzy principles and tools of Matlab. In: *Proceedings of the 2013 International Conference on Systems, Control and Informatics (SCI 2013)*, Venice, 2013, pp. 222-226.
- [Hrehova 2013b] Hrehova, S. Using the graphic tool of Matlab for visualization of input data. *Strojarsstvo Extra*, 2013, Vol. 17, pp. 84 – 85.
- [Krenicky 2011] Krenicky, T. Implementation of Virtual Instrumentation for Machinery Monitoring. In: *Scientific Papers: operation and diagnostics of machines and production systems operational states*. Lüdenscheid: RAM-Verlag, 2011, Vol. 4, pp. 5- 8. ISBN 978-3-942303-10-1
- [Murcinkova 2013] Murcinkova, Z., Krenicky, T. Implementation of virtual instrumentation for multiparametric technical system monitoring. In: *SGEM 2013: 13th Int. Multidisciplinary Sci. Geoconf. Vol. 1: 16-22 June, 2013, Albena, Bulgaria*. Sofia: STEF92 Technology, 2013. pp. 139-144. ISBN 978-954-91818-9-0.
- [Panda 2016] Panda, A., Jurko, J., Pandova, I. *Monitoring and Evaluation of Production Process*. Switzerland: Springer, 2016, pp. 165. ISBN 978-3-319-29441-4
- [Patermarakis 1998] Patermarakis, G. Development of a theory for the determination of the composition of the anodizing solution inside the pores during the growth of porous anodic Al<sub>2</sub>O<sub>3</sub> films on aluminium by a transport phenomenon analysis. *Journal of Electroanalytical Chemistry*, 1998, Vol. 447, pp. 25 - 41.
- [Rahimi 2009] Rahimi, M. H. et al. Study the effect of striping in two-step anodizing process on pore arrangement of nanoporous alumina. In: *Applied Surface Science*, 2009, Vol. 256, pp. 12-16.
- [Tsangaraki-Kaplanogloua 2006a] Tsangaraki-Kaplanogloua, I. et al. Effect of alloy types on the electrolytic coloring process of aluminium. *Surface & Coatings Technology*, 2006, Vol. 200, pp. 3969 – 3979.
- [Tsangaraki-Kaplanogloua 2006b] Tsangaraki-Kaplanogloua, I. et al. Effect of alloy types on the anodizing process of aluminum. *Surface & Coatings Technology*, 2006, Vol. 200, pp. 2634 – 2641.

#### CONTACTS:

PaedDr. Alena Vagaska, PhD.  
 RNDr. Erika Fechova, PhD.  
 Technical University of Kosice  
 Faculty of Manufacturing Technologies with a seat in Presov,  
 Department of Mathematics, Informatics and Cybernetics  
 Bayerova 1, 080 01 Presov, Slovak Republic  
 Tel.: + 421 55 602 6430, + 421 55 602 6421  
 e-mail: alena.vagaska@tuke.sk, erika.fechova@tuke.sk  
<http://www.tuke.sk>

Ing. Peter Michal, PhD.  
 CCTo, a.s.,  
 Dopravna 2, 955 01 Topolcany  
 service: Masarykova 22, 080 01, Presov, Slovak Republic  
 e-mail: michal.peter.pm@gmail.com

Ing. Miroslav Gombar, PhD.  
 doc. Ing. Jan Kmec, CSc.  
 Institute of Technology and Businesses in Ceske Budejovice  
 Department of Mechanical Engineering,  
 Okruzni 10, 370 01 Ceske Budejovice, Czech Republic  
 e-mail: gombar.mirek@gmail.com, kmec@mail.vstecb.cz